CHEMISTRY
A EUROPEAN JOURNAL

DOI: 10.1002/chem.200800309

Conformationally Restricted Dipyrromethene Boron Difluoride (BODIPY) Dyes: Highly Fluorescent, Multicolored Probes for Cellular Imaging

Qingdong Zheng,* Gaixia Xu, and Paras N. Prasad*[a]

Abstract: Novel fluorescent, conformationally restricted dipyrromethene boron difluoride (BODIPY) dyes have been prepared by introducing a naphthalenyl group at the *meso* position of the BODIPY core. These BODIPY dyes exhibit increased fluorescence quantum yields compared with dyes that have a *meso*-position phenyl group with internal rotation. The absorption and emission wavelengths of such conformationally restricted BODIPY dyes can be easily tuned to the near-IR range by derivatization through a condensation reaction with benzaldehyde derivatives. The two-photon absorption properties of these BODIPY dyes were also investigated and the results show that they exhibit increased two-photon excited fluorescence compared to analogue dyes that contain a phenyl group. The one- and two-photon fluorescence imaging of living cells by using selected BODIPY dyes has been successfully demonstrated.

Keywords: dyes/pigments · fluorescent probes · imaging agents · luminescence · two-photon absorption

Introduction

Fluorescence microscopy is one of the most versatile imaging techniques in biomedical research, and allows the noninvasive imaging of cells and tissues with molecule specificity. Consequently, fluorescent probes that have high fluorescence quantum yields and that emit light of various colors are in great demand because of the key role they play in fluorescence microscopy.[1–4] So far, cyanine dyes have attracted much attention in fluorescence imaging, owing to the easy tunability of their absorption and emission wavelengths up to several hundred nm.[5] However, these cyanine chromophores often have low fluorescence quantum yields (less than 10–15%), which limits their applications. In contrast, dipyrromethene boron difluoride (BODIPY) dyes generally have high fluorescence quantum yields as well as intense absorption.[6,7] To label specific biological targets, functional groups can be introduced to the BODIPY core, while retaining their inherent properties. The *meso* position of BODIPY dyes has often been used as a connection into which aryl substitutes with various functionalities can be easily introduced.[8,9] Although arylation at the BODIPY *meso* position does not have much effect on the linear absorption and emission wavelengths, different sterical configurations between the aryl group at the *meso* position and the BODIPY core may greatly affect other photophysical properties of these dyes. For example, the fluorescence quantum yield of *meso*-phenyl compound **PY1** is much less than that of its more substituted analogue **PY2** (Scheme 1).[10,11] At the same time, compound **PY2** shows hypsochromically shifted absorption and emission compared with **PY1**. Such differences are widely attributed to β substituents that prevent free rotation of the phenyl group and, therefore, reduce the loss of energy from excited states via nonirradiative molecular relaxation. The two methyl groups at the β positions also lead to an increase in the dihedral

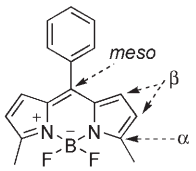

PY1
ϕ = 19% in MeOH
λ_{max} = 508 nm
E_{max} = 521 nm

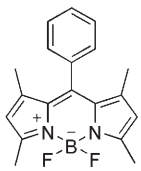

PY2
ϕ = 61% in MeOH
λ_{max} = 498 nm
E_{max} = 508 nm

Scheme 1. Chemical structures and photophysical properties of **PY1** and **PY2**. ϕ is the fluorescence quantum yield, λ_{max} is the linear absorption spectrum maximum, and E_{max} is the linear emission spectrum maximum.

[a] Dr. Q. Zheng, Dr. G. Xu, Prof. Dr. P. N. Prasad
Department of Chemistry
Institute for Lasers, Photonics, and Biophotonics
State University of New York at Buffalo
Buffalo, NY 14260 USA
Fax: (+1) 716-645-6945
E-mail: qzheng7@jhu.edu
pnprasad@buffalo.edu

angle between the BODIPY core and the phenyl group, which results in blue-shifted absorption and emission spectra.[12] These results suggest that the introduction of a more bulky aryl group, such as a naphthalenyl group, may further increase the fluorescence quantum yields for these kinds of dyes because free rotation of the naphthalenyl group would be more difficult.

With this consideration in mind, we report herein the design and synthesis of two conformationally restricted BODIPY dyes (**2a**,**b**) through the introduction of a naphthalenyl group at the *meso* position. For comparison purposes, we also prepared two phenyl-substituted analogues (**1a**,**b**). In addition, an attempt was made to tune the emission wavelengths of these conformationally restricted BODIPY dyes to the near-IR range by derivatization through condensation between the methyl groups at the α positions and a substituted benzaldehyde. The linear and nonlinear photophysical properties of these BODIPY dyes were also investigated. Finally, the one- and two-photon cellular imaging of cancer cells was demonstrated with the aid of selected BODIPY dyes.

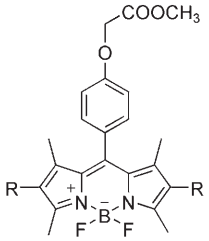

1a: R = H
1b: R = CH_2CH_3

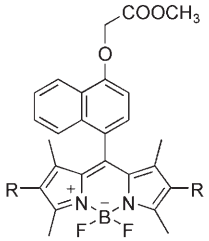

2a: R = H
2b: R = CH_2CH_3

Results and Discussion

Synthesis: As depicted in Scheme 2, compounds **1** and **2** were synthesized in yields of 35 to 45% by reacting aldehydes with 3-ethyl-2,4-dimethylpyrrole (or 2,4-dimethylpyrrole) in the presence of trifluoroacetic acid (TFA) and 2,3-dichloro-5,6-dicyano-1,4-benzoquinone (DDQ), followed by the addition of $BF_3{\cdot}OEt_2$. As shown in Scheme 3, compounds **3** and **4** were prepared by a Knoevenagel-type condensation reaction between **2b** and 4-dimethylaminobenzaldehyde in the presence of acetic acid, piperidine, and molecular sieves in toluene. The products resulting from the single and double condensation reactions could be separated by using column chromatography with dichloromethane as the eluent. All new

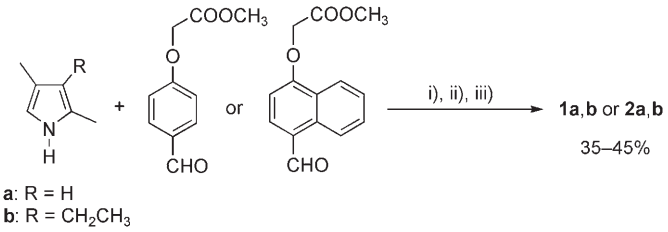

a: R = H
b: R = CH_2CH_3

Scheme 2. Synthesis of BODIPY dyes **1a**,**b** and **2a**,**b**. i) TFA, CH_2Cl_2, 12 h, RT; ii) DDQ; iii) NEt_3, $BF_3{\cdot}OEt_2$.

compounds were confirmed by ^1H and ^{13}C NMR spectroscopy, HRMS, and elemental analysis.

Crystal structures of 1a and 2a: Crystals suitable for X-ray analysis were grown by slow evaporation of *n*-hexane into a solution of **1a** or **2a** in dichloromethane. Cell parameters and refinement details are summarized in Table 1. Note that there is only one crystallographically independent molecule in **1a**, whereas there are two crystallographically independent molecules in **2a**. Figure 1 shows that the angles of N1-B1-N2 and F1-B1-F2 in both compounds indicate a tetrahedral BF_2N_2 configuration, and are within the range of the published data.[13,14] The average bond length of N1−C1 indicates double-bond character, compared with the single-bond character of N1−C4. For both compounds, there is strong π-electron delocalization between the central six-membered ring and the two adjacent pyrrole rings. However, almost no π-electron delocalization is observed between the aryl group at the *meso* position and the BODIPY core (indacene plane), as indicated by the average length of the C5−C14 bond, which is almost the same length as a single C−C bond. Figure 2 shows how the structures of **1a** and **2a** are stabilized by π–π and C−H···π interactions.

It can be seen from the crystal structures that the indacene planes of **1a** and **2a** are essentially planar. For both compounds, the deviation of the pyrrole planes with respect to each other and the central ring is typically only a few degrees. However, the indacene plane is almost perpendicular to the aryl group at the *meso* position. On examining the dihedral angle between the phenyl/naphthalenyl group and in-

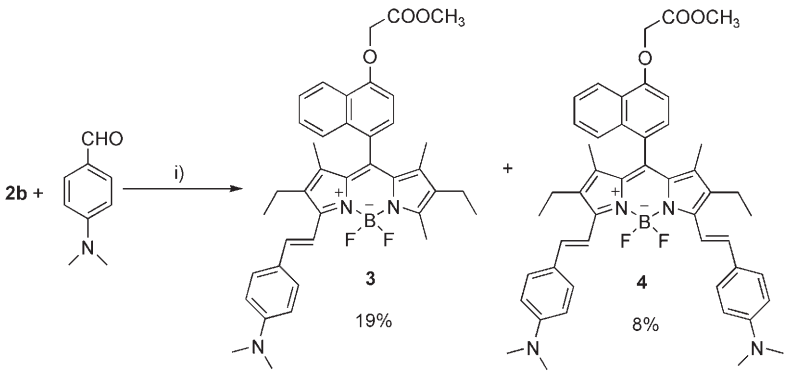

Scheme 3. Synthesis of monostyryl- and distyryl-BODIPY dyes **3** and **4**. i) Piperidine, AcOH, toluene, and molecular sieves, reflux, 24 h.

Table 1. Crystallographic data and structure refinement for **1a** and **2a**.[a]

	1a	**2a**
formula	$C_{22}H_{23}BF_2N_2O_3$	$C_{52}H_{50}B_2F_4N_4O_6$
M_r	412.23	924.58
cell system, space group	triclinic, $P\bar{1}$	monoclinic, $P2_1/c$
T [K]	90(2)	90(2)
a [Å]	10.5126(9)	14.8040(6)
b [Å]	10.628(1)	21.718(1)
c [Å]	10.762(1)	16.782(1)
α [°]	102.117(2)	90.00
β [°]	101.129(1)	123.061(3)
γ [°]	116.535(2)	90.00
V [Å^3]	993.7(2)	4522.0(3)
Z	2	4
ρ_{calcd} [Mg m^{-3}]	1.378	1.358
μ [mm^{-1}]	0.10	0.10
R_{int}	0.042	0.056
θ_{max} [°]	29.6	26.0
R [$F^2 > 2\sigma(F^2)$]	0.037	0.067
$wR(F^2)$	0.104	0.192
S	1.02	1.02
no. of reflns	5597	8896
no. of params	305	613
$(\Delta/\sigma)_{max}$	0.002	<0.0001
$\Delta\rho_{max}$, $\Delta\rho_{min}$ [e Å^{-3}]	0.41, −0.22	0.90, −0.90

[a] Criterion for observed reflections: $I > 2\sigma(I)$. Refinement on F^2.

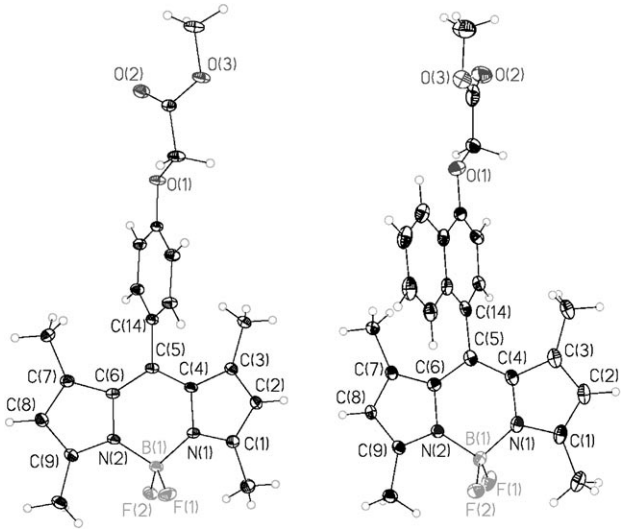

Figure 1. Perspective views of **1a** (left) and **2a** (right), showing 50% probability displacement ellipsoids. Selected bond lengths [Å] and angles [°] for **1a**: F−B1 1.402(2), F2−B1 1.393(1), N1−C1 1.346(1), N1−C4 1.405(1), N1−B1 1.545(1), C1−C2 1.406(1), C2−C3 1.383(1), C3−C4 1.431(1), C4−C5 1.396(1), C5−C14 1.496(1), F2-B1-F1 108.67(8), F2-B1-N2 110.49(9), F1-B1-N2 110.39(9), F2-B1-N1 110.65(9), F1-B1-N1 110.10(9), N2-B1-N1 106.52(8); selected bond lengths [Å] and angles [°] for **2a**: F1−B1 1.398(3), F2−B1 1.386(3), N1−C1 1.349(3), N1−C4 1.403(4), N1−B1 1.549(4), C1−C2 1.405(4), C2−C3 1.379(4), C3−C4 1.432(4), C4−C5 1.398(4), C5−C14 1.489(4), F2-B1-F1 109.0(2), F2-B1-N2 110.9(2), F1-B1-N2 110.0(2), F2-B1-N1 111.1(2), F1-B1-N1 109.3(2), N2-B1-N1 106.6(2).

dacene plane, we find a dihedral angle of 82.4(1)° in **1a**, whereas in **2a** this angle is 78.0(3) or 79.2 (3)°. The introduction of a naphthalenyl group leads to a small reduction in the dihedral angle between the aryl group and indacene plane, and a slight decrease in the C5−C14 bond length between the aryl group and indacene plane, from 1.496(1) Å in **1a** to 1.489(4) Å in **2a**.

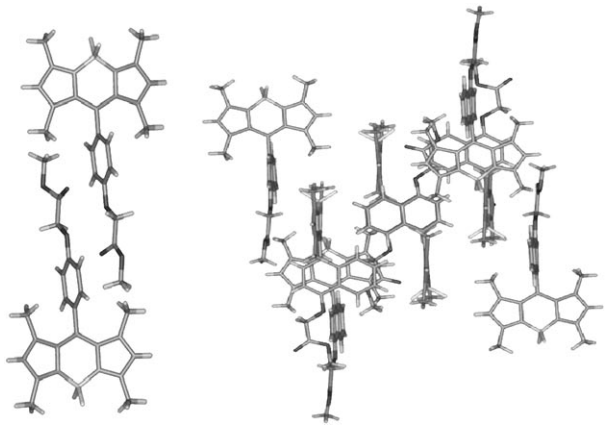

Figure 2. Molecular packing in the crystal structures of **1a** (left) and **2a** (right).

Linear absorption and emission spectra: Linear absorption spectra for compounds **1**–**4** in toluene were recorded on a Shimadzu UV-3101 PC spectrophotometer. One-photon excited fluorescence spectra were measured in dilute solutions by using a Jobin–Yvon FluoroLog-3 (model FL-3-11) spectrofluorometer and 10 mm path-length cuvettes. The fluorescence lifetimes for these compounds were measured by using a high-speed streak camera with a resolution of 20 ps.

Table 2 summarizes the linear and two-photon absorption (TPA) properties for **1a**,**b** and **2a**,**b** in toluene and shows the linear absorption maxima, molar extinction coefficients, emission maxima, Stokes shifts, fluorescence quantum yields, fluorescence lifetimes, TPA peak, and TPA cross-section peak values. Figure 3 depicts the linear absorption and emission spectra for **1a**,**b** and **2a**,**b** in toluene. As shown in the figures, the linear absorption and emission spectra for dilute **1a**,**b** and **2a**,**b** in toluene are quite similar, except that **2a** and **2b** exhibit 3 nm red-shifted linear absorption and

Table 2. Photophysical properties of compounds **1**–**4** in toluene.

	$\varepsilon_{max}\times10^5$ [M^{-1}cm^{-1}]	λ_{max} [nm]	E_{max} [nm]	$\Delta\nu$[a] [cm^{-1}]	ϕ[b] [%]	τ[c] [ns]	λ^2_{max}[d] [nm]	δ_{TPA}[e] [GM]
1a	0.97	504	517	498.9	60	3.7	950	82
2a	1.00	507	520	493.1	98	5.8	950	112
1b	0.94	527	542	525.1	78	5.1	990	109
2b	0.95	530	545	519.3	99	7.0	990	128
3	1.03	624	658	828.1	64	3.8	–	–
4	1.05	714	752	707.7	40	2.8	–	–

[a] Stokes shift. [b] Fluorescence quantum yield. Rhodamine 6G (94% in methanol) was used as a reference for **1a**,**b** and **2a**,**b**,[15] Cresyl Violet (54% in methanol) was used as a reference for **3**,[16] and Nile Blue (26% in ethylene glycol) was used as a reference for **4**.[17] [c] Fluorescence lifetime, recorded at a resolution of 20 ps. [d] TPA peak wavelength. [e] TPA cross-section peak value, 1 GM = 10^{-50} cm^{4}s per photon, experimental uncertainty ±15%.

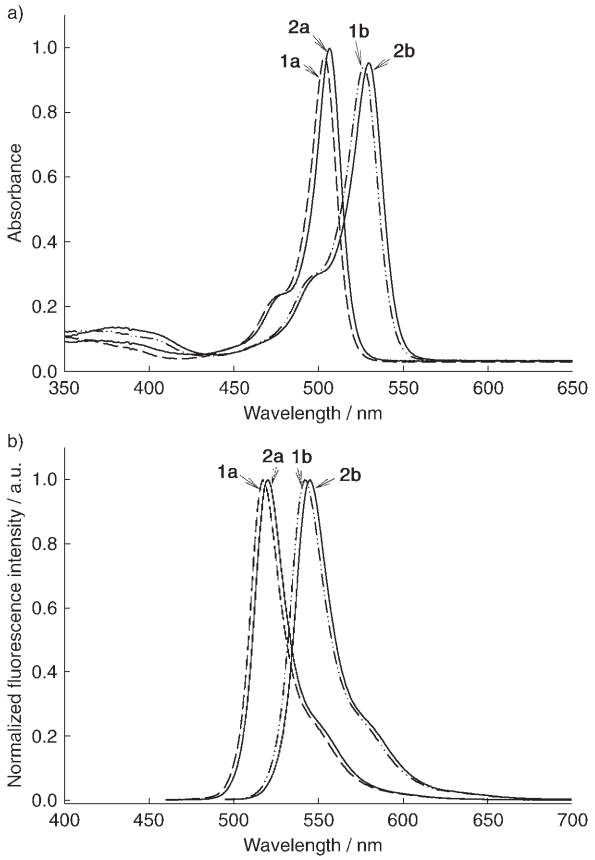

Figure 3. a) Linear absorption (10^{-5} M) and b) emission (10^{-6} M) spectra of **1a**,**b** and **2a**,**b** in toluene.

emission spectra. By examining the geometric arrangements of **1a** and **2a**, one can see that the phenyl/naphthalenyl group and the indacene plane are almost perpendicular to each other, and that the dihedral angle between the phenyl group and indacene plane (**1a**) is around 3 or 4° greater than the angle between the naphthalenyl group and indacene plane (**2a**), which may contribute to the bathochromically shifted absorption and emission spectra observed for chromophores that contain a naphthalenyl group. Furthermore, the introduction of a 5-membered heteroaromatic ring, such as a furan ring, at the *meso* position of the BODIPY core leads to a decrease in the dihedral angle and results in red-shifted linear absorption and emission spectra; these results will be published elsewhere. However, compounds **2a** and **2b** have higher fluorescence quantum yields (98 and 99% for **2a** and **2b**, respectively) compared with **1a** and **1b** (60 and 78% for **1a** and **1b**, respectively). The only difference between **1a** and **2a** is the aryl group at the *meso* position. From the crystal structures we know that these aryl groups are actually perpendicular to the indacene plane. It has been shown that the excited state of an aryl-substituted BODIPY dye has a second, lower-energy minimum in which the nonhindered aryl group rotates closer to the mean plane of the BODIPY core, which itself undergoes some distortion. This relaxed, distorted, excited-state conformation has low radiative probability,[12] and is energetically less accessible in a BODIPY dye that has a more conformationally restricted group in the *meso* position. Obviously, the naphthalenyl group is more sterically hindered than the phenyl group, which is the main reason that **2a** has a fluorescence quantum yield that is 63% greater than **1a**. This explanation is also valid in the case of **1b** and **2b**. The quantum yield of **2b** in toluene is close to 100%, which is 27% greater than that of **2a**. To explore the fluorescence dynamics of these chromophores, their fluorescence decay profiles in toluene were collected. The fluorescence decay traces of these chromophores could all be fitted by a single-exponential curve, and the fitting results are listed in Table 2. The naphthalenyl-containing **2a** and **2b** have longer fluorescence lifetimes compared with their phenyl analogues **1a** and **1b**. For example, compound **2a** has a fluorescence lifetime of 5.8 ns, whereas compound **1a** has a fluorescence lifetime of 3.7 ns. Compounds **1** and **2** have a small Stokes shift in the range of 493 to 525 cm^{-1}. The monostyryl compound **3** and the distyryl compound **4** are both derived from **2b**. As shown in Figure 4, compound **3** has a linear absorption maximum at

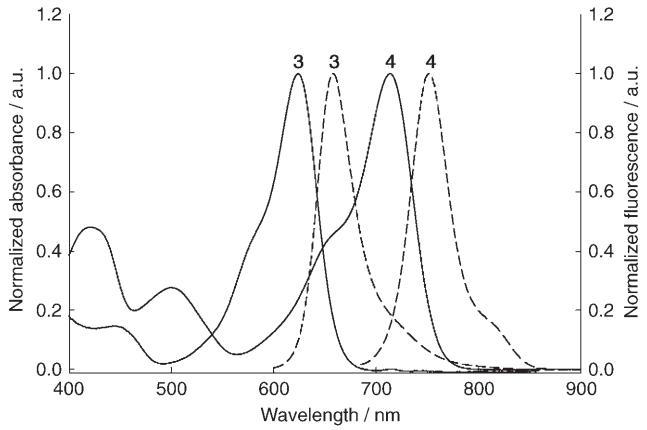

Figure 4. Linear absorption (——; 10^{-5} M) and emission (– – –; 10^{-6} M) spectra of **3** and **4** in toluene.

$\lambda = 624$ nm and an emission maximum at $\lambda = 658$ nm. The linear absorption band of **4** is centered at $\lambda = 714$ nm, and the emission peak is located at $\lambda = 752$ nm. An extra styryl group leads to more red-shifted linear absorption and emission spectra. The fluorescence quantum yields for **3** and **4** are 63 and 40%, respectively. Although these values are smaller than the value for **2b**, they are much higher than the values for general cyanine dyes (<10–15%).[5] At the same time, compounds **3** and **4** show decreased fluorescence lifetimes compared with **2b**, which is probably due to their elongated π-conjugated system.

Two-photon absorption and emission spectroscopy: There has been a lot of research focused on the development of materials with large TPA and high fluorescence quantum yields owing to their applications in two-photon bioimaging and two-photon biosensing.[18–22] In Figure 3a, one can see

that **1a**,**b** and **2a**,**b** have no linear absorption above $\lambda =$ 600 nm. However, when these chromophores were excited by a focused IR laser beam ($\lambda = 730$–1050 nm), we observed strong frequency up-converted fluorescence. As shown in Figure 5, the fluorescence spectrum for each compound is

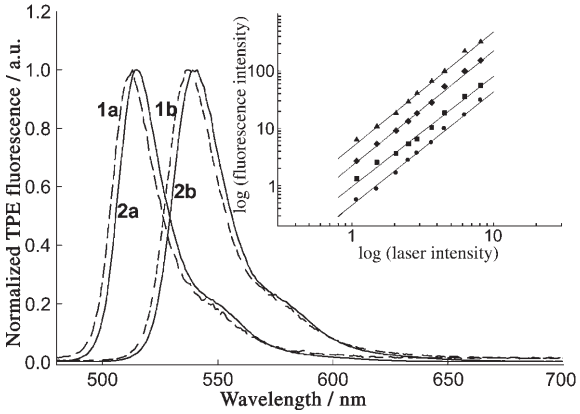

Figure 5. Main graph: TPE fluorescence spectra for **1a**,**b** and **2a**,**b** (10^{-4} M in toluene). Inset: Fluorescence peak intensities versus laser intensity at $\lambda = 950$ nm. ●: **1a**, slope = 1.98; ■: **2a**, slope = 1.93; ◆: **1b**, slope = 2.01; ▲: **2b**, slope = 2.02. These results demonstrate two-photon absorption.

exactly the same as that induced by one-photon excitation, which indicates that this fluorescence is from the same fluorescing excited state. However, measurements from laser-intensity dependence studies of the fluorescence of **1a**,**b** and **2a**,**b** showed that the fluorescence results from TPA, because the emission intensity depends quadratically on the excitation power (Figure 5, inset). Owing to the high fluorescence quantum yields of these chromophores, the TPA spectra for **1a**,**b** and **2a**,**b** can be readily obtained by using the two-photon excited (TPE) fluorescence method.[23] The TPA action cross-section ($\phi\delta$) spectra for **1a**,**b** and **2a**,**b** are shown in Figure 6. The TPA maximium is at $\lambda = 950$ nm for both **1a** and **2a** (Figure 6a), which is a little less than twice the wavelength of linear λ_{max}. However, compound **2a** has an $\phi\delta$ peak value of 110 GM, which is 124% larger than the value for **1a** (49 GM). One can see from Table 2 that the fluorescence quantum yields for **1a** and **2a** are 60 and 98%, respectively. Accordingly, compounds **1a** and **2a** have TPA cross-sections of 82 and 112 GM, respectively. Similarly, compound **2b** has an $\phi\delta$ peak value of 127 GM at $\lambda =$ 990 nm, which is 49% larger than the value for **1b** (85 GM at $\lambda = 990$ nm). The fluorescence quantum yields for compounds **1b** and **2b** are 78 and 99%, respectively. Therefore, compounds **1b** and **2b** have TPA cross-sections of 109 and 128 GM, respectively. A comparison between compounds **1a** and **2a** and compounds **1b** and **2b** shows that ethyl substitutions at the two β positions of the BODIPY core lead to a bathochromically shifted TPA band and an increased TPA peak value.

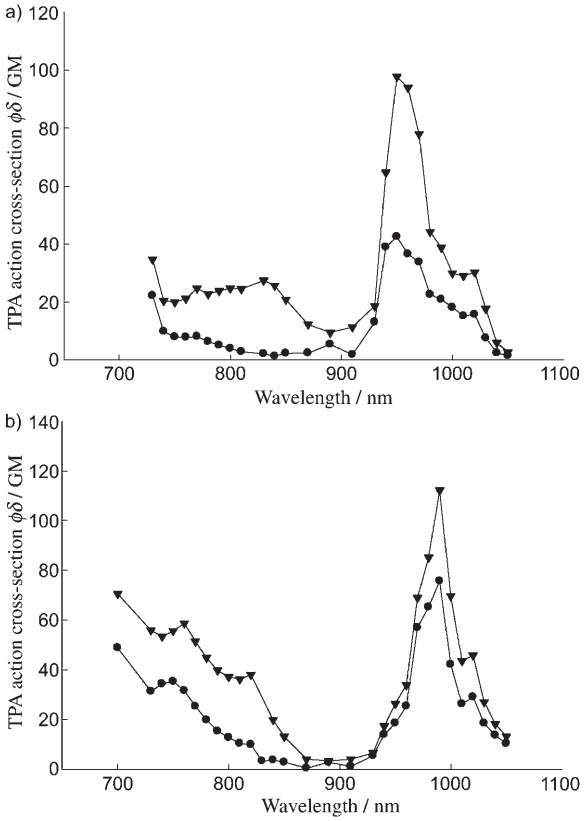

Figure 6. Two-photon excitation spectra for a) **1a** (●) and **2a** (▼) and b) **1b** (●) and **2b** (▼) in toluene.

Selected compounds for cellular imaging: To test the practical applicability of these highly fluorescent probes, HeLa (human cervix epitheloid carcinoma) cells were treated with **2b**, **3**, and **4** in water (containing 0.1% dimethylsulfoxide, DMSO). Figure 7a, b, and c shows confocal microscopy images of HeLa cells stained with **2b**, **3**, and **4**, respectively, and were obtained by excitation with $\lambda = 514$, 543, and 643 nm lasers, respectively. Figure 7, middle shows the corresponding transmission images, and Figure 7, bottom shows the overlays of the fluorescence and transmission images. As can be seen in the images, these molecules can be easily taken up by the cells. We did not observe any signs of morphological damage to the cells upon treatment with these chromophores for 2 to 4 h, which demonstrates their nontoxicity. As shown herein, with chemical modification of these conformationally restricted BODIPY dyes, tuning of the fluorescence activity across the visible and into the near-IR spectrum was achieved. These probes can be easily conjugated with biomacromolecules, such as antibodies and DNAs, because they all contain acetic acid methyl ester groups that can be converted into acetic acid groups by a simple hydrolysis reaction.

Significant TPE fluorescence was observed from **2b** as a result of its high fluorescence quantum yield, although its TPA cross-section is only moderate. Therefore, two-photon scanning microscopy imaging was carried out on HeLa cells treated with **2b**. Figure 8a shows the two-photon scanning

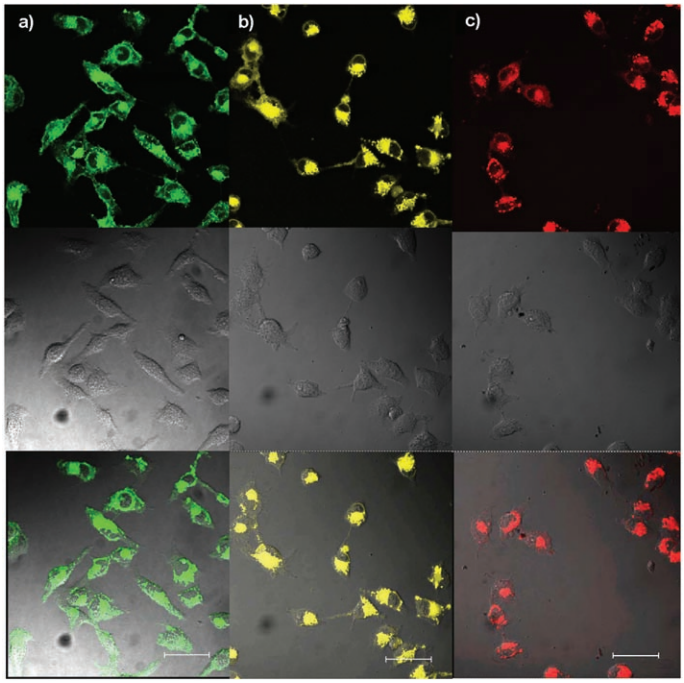

Figure 7. Top: Confocal microscopic images of HeLa cells treated with a) **2b**, b) **3**, and c) **4**. Confocal microscopy images were obtained by using laser excitation at $\lambda = 514$ (**2b**), 543 (**3**), and 643 nm (**4**). Middle: The corresponding transmission images. Bottom: Overlays of the fluorescence and transmission images. All scale bars are 47.62 μm long.

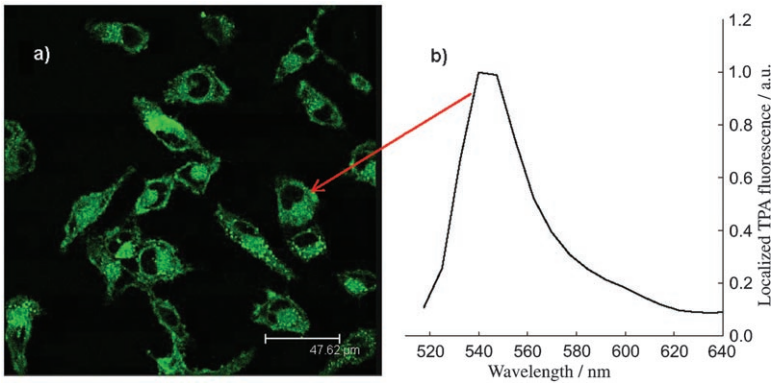

Figure 8. a) Two-photon confocal microscopic image and b) localized spectrum of the TPE fluorescence of HeLa cells treated with **2b**. Confocal microscopy image and two-photon fluorescence were obtained by using laser excitation at $\lambda = 1028$ nm. The scale bar is 47.62 μm long.

microscopy image, and Figure 8b depicts the localized spectrum of TPE fluorescence in cells treated with **2b** and DMSO (0.1%) in water and excited by a laser at $\lambda =$ 1028 nm. Compared with UV/Vis-excited imaging, this two-photon imaging technique leads to the possibility of long-term imaging of cellular processes and deep tissue penetration, and causes less photodamage because of the long-wavelength excitation. These features enhance the potential of BODIPY dyes for biological applications in multiplex imaging and multiphoton microscopy, especially for complex multi-imaging tasks.[22]

Conclusions

Novel fluorescent BODIPY dyes have been synthesized by introducing a naphthalenyl group at the *meso* position of the BODIPY core. A condensation reaction between 4-dimethylaminobenzaldehyde and a methyl group at the α position of the BODIPY core afforded chromophores that emitted in the red-color and near-IR regions. All new compounds were characterized by using ^{1}H and ^{13}C NMR spectroscopy, HRMS, and elemental analysis. Compounds **1a** and **2a** were further characterized by X-ray diffraction to study the structure–property relationship of this class of dyes. BODIPY dyes that had a naphthalenyl group at the *meso* position exhibited increased fluorescence quantum yields and longer excited-state lifetimes compared with those that had a phenyl group at the *meso* position. This effect is attributed to a reduction in the loss of energy from nonirradiative molecular relaxation of the excited state for chromophores with a naphthalenyl group because free rotation is more difficult for a naphthalenyl group than for a phenyl group. The red and near-IR spectrum BODIPY dyes exhibit higher fluorescence quantum yields compared with common cyanine dyes. The two-photon excitation spectra of **1a**,**b** and **2a**,**b** show that conformationally restricted BODIPY dyes show increased TPE emission spectra compared with dyes that have a phenyl group at the *meso* position. The one- and two-photon fluorescence imaging of living cells was successfully demonstrated by using selected BODIPY dyes. This work presents a novel type of optical probe for biological applications, such as multiplex imaging and multiphoton microscopy.

Experimental Section

Materials and instruments: All chemicals were purchased from Aldrich and were used without further purification. ^{1}H and ^{13}C NMR spectra were recorded on an Inova-500 spectrometer (500 MHz) and a Gemini-300 (75 MHz), respectively. Elemental analysis was carried by Atlantic Analysis Inc., Norcross, GA (USA). The linear absorption spectra of dilute solutions (10^{-5} M in toluene) were recorded by using a Shimadzu UV-3101 PC spectrophotometer.

(4-Formylphenoxy)acetic acid methyl ester:[24] Anhydrous K_2CO_3 (17 g, 123 mmol) was added to a solution of 4-hydroxybenzaldehyde (10 g, 82 mmol) in dry acetone (120 mL), then ethyl bromoacetate (10.9 mL, 120 mmol) was added dropwise at room temperature. The mixture was heated at reflux for 4 h, then filtered and the solvent was removed under reduced pressure. The residue was dissolved in AcOEt (50 mL), then washed with NaOH (2 N) and water. The organic layer was dried over anhydrous Na_2SO_4, filtered, and the solvent was removed under reduced pressure to give the title compound as a white solid that was sufficiently pure to be used in the following step (9.5 g, 45.7 mmol, 92%). ^{1}H NMR

(500 MHz, $CDCl_3$, 25 °C, TMS): $\delta = 9.90$ (s, 1H), 7.85 (d, $J = 9.0$ Hz, 2H), 7.01 (d, $J = 9.0$ Hz, 2H), 4.73 (s, 2H), 3.82 ppm (s, 3H); ^{13}C NMR (125 MHz, $CDCl_3$, 25 °C, TMS): $\delta = 190.6$, 168.5, 162.6, 131.9, 130.9, 114.9, 65.1, 52.4 ppm.

4-Formylnaphthalene-1-yloxyacetic acid methyl ester:[25] The synthesis of this precursor is analogous to that of (4-formylphenoxy)acetic acid methyl ester (92%). ^1H NMR (500 MHz, $CDCl_3$, 25 °C, TMS): $\delta = 10.22$ (s, 1H), 9.29 (d, $J = 8.0$ Hz, 1H), 8.43 (d, $J = 8.0$ Hz, 1H), 7.89 (d, $J = 8.0$ Hz, 1H), 7.72 (t, $J = 8.0$ Hz, 1H), 7.61 (t, $J = 8.0$ Hz, 1H), 6.79 (d, $J = 8.0$ Hz, 1H), 4.92 (s, 2H), 3.85 ppm (s, 3H); ^{13}C NMR (75 MHz, $CDCl_3$, 25 °C, TMS): $\delta = 192.2$, 168.3, 138.8, 131.9, 129.8, 126.7, 125.8, 125.4, 124.8, 122.5, 103.6, 65.4, 52.5 ppm.

General procedure for the preparation of 1a,b and 2a,b: Benzaldehyde (5 mmol) and 2,4-dimethylpyrrole (10 mmol) were dissolved in dry CH_2Cl_2 (250 mL) under an argon atmosphere. One drop of TFA was added and the solution was stirred overnight at room temperature. After complete consumption of the aldehyde (monitored by TLC; silica, CH_2Cl_2 eluent), a solution of DDQ (5 mmol) in CH_2Cl_2 was added with stirring. Triethylamine (14.3 mmol) was added to the resulting solution, followed by $BF_3{\cdot}OEt_2$ (19.8 mmol). The mixture was stirred for 40 min, then washed with water. The aqueous solution was extracted with CH_2Cl_2, and the combined organic fractions were dried over Na_2SO_4, filtered, and the solvent evaporated under reduced pressure. The crude compound was purified by flash chromatography (silica gel, CH_2Cl_2 eluent).

*1,3,5,7-Tetramethyl-8-(4-methoxycarbonylmethyloxyphenyl)-4,4′-difluoroboradiazaindacene (**1a**)*: Red crystalline solid (0.72 g, 35%). ^1H NMR (500 MHz, $CDCl_3$, 25 °C, TMS): $\delta = 7.20$ (d, $J = 8.5$ Hz, 2H), 7.03 (d, $J = 8.5$ Hz, 2H), 5.98 (s, 2H), 4.70 (s, 2H), 3.83 (s, 3H), 2.55 (s, 6H), 1.41 ppm (s, 6H); ^{13}C NMR (75 MHz, $CDCl_3$, 25 °C, TMS): $\delta = 168.9$, 158.3, 155.4, 143.1, 141.3, 131.7, 129.4, 128.2, 121.2, 115.3, 65.3, 52.3, 14.6, 14.5 ppm; HRMS: m/z: calcd for $C_{22}H_{23}BF_2N_2O_3$: 412.1764; found: 412.1769; elemental analysis calcd (%) for $C_{22}H_{23}BF_2N_2O_3$: C 64.10, H 5.62, N 6.80; found: C 64.13, H 5.63, N 6.80.

*2,6-Diethyl-1,3,5,7-tetramethyl-8-(4-methoxycarbonylmethyloxyphenyl)-4,4′-difluoroboradiazaindacene (**1b**)*: Red crystalline solid (0.87 g, 37%). ^1H NMR (500 MHz, $CDCl_3$, 25 °C, TMS): $\delta = 7.19$ (d, $J = 8.5$ Hz, 2H), 7.02 (d, $J = 8.5$ Hz, 2H), 4.71 (s, 2H), 3.83 (s, 3H), 2.53 (s, 6H), 2.30 (q, $J = 7.5$ Hz, 4H), 1.31 (s, 6H), 0.98 ppm (t, $J = 7.5$ Hz, 6H); ^{13}C NMR (75 MHz, $CDCl_3$, 25 °C, TMS): $\delta = 169.0$, 158.2, 153.6, 139.7, 138.3, 132.7, 131.0, 129.6, 129.1, 115.2, 65.3, 52.3, 17.0, 14.6, 12.5, 11.8 ppm; HRMS: m/z: calcd for $C_{26}H_{31}BF_2N_2O_3$: 468.2390; found: 468.2391; elemental analysis calcd (%) for $C_{26}H_{31}BF_2N_2O_3$: C 66.68, H 6.67, N 5.98; found: C 66.50, H 6.62, N 6.00.

*1,3,5,7-Tetramethyl-8-(4-methoxycarbonylmethyloxynaphthalen-1-yl)-4,4′-difluoroboradiazaindacene (**2a**)*: Dark red crystalline solid (0.88 g, 38%). ^1H NMR (500 MHz, $CDCl_3$, 25 °C, TMS): $\delta = 8.42$ (d, $J = 8.5$ Hz, 1H), 7.73 (d, $J = 8.5$ Hz, 1H), 7.54 (t, $J = 7.5$ Hz, 1H), 7.47 (t, $J = 7.5$ Hz, 1H), 7.26 (s, 1H), 6.81 (d, $J = 8.0$ Hz, 1H), 5.93 (s, 2H), 4.89 (s, 2H), 3.86 (s, 3H), 2.58 (s, 6H), 1.10 ppm (s, 6H). ^{13}C NMR (75 MHz, $CDCl_3$, 25 °C, TMS): $\delta = 168.8$, 155.5, 154.5, 143.0, 140.1, 132.8, 132.3, 128.0, 126.3, 125.7, 124.7, 122.4, 121.1, 104.8, 65.6, 52.3, 14.6, 14.0 ppm; HRMS: m/z: calcd for $C_{26}H_{25}BF_2N_2O_3$: 462.1921; found: 462.1926; elemental analysis calcd (%) for $C_{26}H_{25}BF_2N_2O_3$: C 67.55, H 5.45, N 6.06; found: C 67.55, H 5.46, N 6.01.

*2,6-Diethyl-1,3,5,7-tetramethyl-8-(4-methoxycarbonylmethyloxynaphthalen-1-yl)-4,4′-difluoroboradiazaindacene (**2b**)*: Dark red crystalline solid (1.17 g, 45%). ^1H NMR (500 MHz, $CDCl_3$, 25 °C, TMS): $\delta = 8.42$ (d, $J = 8.5$ Hz, 1H), 7.75 (d, $J = 8.5$ Hz, 1H), 7.54 (t, $J = 7.5$ Hz, 1H), 7.46 (t, $J = 7.5$ Hz, 1H), 7.26 (s, 1H), 6.81 (d, $J = 8.0$ Hz, 1H), 4.90 (s, 2H), 3.87 (s, 3H), 2.56 (s, 6H), 2.25 (q, $J = 7.5$ Hz, 4H), 1.01 (s, 6H), 0.94 ppm (t, $J = 7.5$ Hz, 6H); ^{13}C NMR (75 MHz, $CDCl_3$, 25 °C, TMS): $\delta = 168.9$, 154.3, 153.7, 138.4, 138.2, 133.0, 132.6, 131.6, 127.9, 126.6, 126.2, 125.8, 125.6, 125.0, 122.3, 104.8, 65.6, 52.3, 17.0, 14.6, 12.5, 11.2 ppm; HRMS: m/z: calcd for $C_{30}H_{33}BF_2N_2O_3$: 518.2547; found: 518.2549; elemental analysis calcd (%) for $C_{30}H_{33}BF_2N_2O_3$: C 69.51, H 6.42, N 5.40; found: C 69.40, H 6.36, N 5.35.

Monostyryl- and distyryl-BODIPY dyes (3 and 4): 4-Dimethylaminobenzaldehyde (0.29 g, 2 mmol), **2b** (0.52 mg, 1 mmol), glacial acetic acid (0.7 mL), and piperidine (0.8 mL) were heated at reflux for 24 h in dry toluene (50 mL) in the presence of a small amount of activated 4 Å molecular sieves. The mixture was cooled to room temperature, the solvents were removed under reduced pressure, and the crude product was placed on a silica column and eluted with methylene chloride. The blue-colored fraction was collected and recrystallized from methylene chloride/methanol to give **3** as a glossy red powder (0.123 g, 19%), and the green-colored fraction was collected and the solvent was removed under reduced pressure to give **4** as a black crystalline solid (0.062 g, 8%).

*Monostyryl-BODIPY **3***: ^1H NMR (500 MHz, $CDCl_3$, 25 °C, TMS): $\delta = 8.42$ (d, $J = 8.5$ Hz, 1H), 7.78 (d, $J = 8.5$ Hz, 1H), 7.61 (d, $J = 16.5$ Hz, 1H), 7.55–7.50 (m, 3H), 7.46 (t, $J = 7.5$ Hz, 1H), 7.28 (s, 1H), 7.20 (d, $J = 16.5$ Hz, 1H), 6.81 (d, $J = 7.5$ Hz, 1H), 6.71 (d, $J = 9.0$ Hz, 2H), 4.91 (s, 2H), 3.87 (s, 3H), 3.02 (s, 6H), 2.60 (s, 3H), 2.56–2.53 (m, 2H), 2.28–2.22 (m, 2H), 1.10 (t, $J = 7.5$ Hz, 3H), 1.03 (s, 3H), 1.01 (s, 3H), 0.95 ppm (t, $J = 7.5$ Hz, 3H); ^{13}C NMR (125 MHz, $CDCl_3$, 25 °C, TMS): $\delta = 169.0$, 154.2, 150.8, 136.2, 133.3, 128.7, 127.8, 127.0, 126.2, 126.1, 125.8, 125.6, 125.2, 122.2, 112.2, 104.8, 65.6, 52.4, 40.3, 18.4, 17.1, 14.6, 14.0, 11.3, 11.0 ppm; HRMS: m/z: calcd for $C_{39}H_{42}BF_2N_3O_3$: 649.3396; found: 649.3390; elemental analysis calcd (%) for $C_{39}H_{42}BF_2N_3O_3$: C 72.11, H 6.52, N 6.47; found: C 71.96, H 6.49, N 6.42.

*Distyryl-BODIPY **4***: ^1H NMR (500 MHz, $CDCl_3$, 25 °C, TMS): $\delta = 8.43$ (d, $J = 8.0$ Hz, 1H), 7.81 (d, $J = 8.0$ Hz, 1H), 7.67 (d, $J = 16.0$ Hz, 2H), 7.56–7.52 (m, 4H), 7.46 (t, $J = 8.0$ Hz, 1H), 7.29–7.27 (m, 4H), 7.21 (d, $J = 16.0$ Hz, 2H), 6.81 (d, $J = 8.0$ Hz, 1H), 6.75 (d, $J = 8.0$ Hz, 2H), 4.91 (s, 2H), 3.87 (s, 3H), 3.03 (s, 12H), 2.55–2.52 (m, 4H), 1.11 (t, $J = 7.5$ Hz, 6H), 1.03 ppm (s, 6H); ^{13}C NMR (75 MHz, $CDCl_3$, 25 °C, TMS): $\delta = 169.2$, 154.6, 150.7, 136.1, 130.6, 128.8, 126.1, 125.4, 122.2, 116.2, 112.3, 104.8, 65.7, 52.3, 40.4, 17.9, 14.0, 11.0 ppm; HRMS: m/z: calcd for $C_{48}H_{51}BF_2N_4O_3$: 780.4017; found: 780.4026; elemental analysis calcd (%) for $C_{48}H_{51}BF_2N_4O_3$: C 73.84, H 6.58, N 7.18; found: C 73.39, H 6.72, N 7.04.

X-Ray crystallography: A crystal of **1a** or **2a** was mounted on the diffractometer, and data were collected at 90 K. The reflection intensities were collected by using a Bruker APEX II CCD diffractometer installed at a rotating anode source ($Mo_{K\alpha}$ radiation, $\lambda = 0.71073$ Å) and equipped with an Oxford Cryosystems nitrogen flow apparatus. The collection method involved 0.3° scans in ω at 20° in 2θ. Data integration up to a resolution of 0.70 Å was carried out by using SAINT V7.34[26a] with reflection spot size optimization. Absorption corrections were made with the program SADABS.[26a] The structure was solved by using the direct methods procedure and refined by using least-squares methods against F^2 with SHELXS-97 and SHELXL-97.[26b] Nonhydrogen atoms were refined anisotropically, and hydrogen atoms were allowed to ride on the respective atoms. Crystal data and details of the data collection and refinement for **1a** and **2a** are summarized in Table 1. CCDC-678553 (**1a**) and -678554 (**2a**) contain the supplementary crystallographic data for this paper. These data can be obtained free of charge from The Cambridge Crystallographic Data Centre via www.ccdc.cam.ac.uk/data_request/cif.

Fluorescence properties and fluorescence quantum yields: Steady-state fluorescence spectroscopic studies were performed by using a Jobin–Yvon Fluorolog-3 (model FL-3-11) spectrofluorometer. The relative quantum yields of fluorescence of **1a**,**b** and **2a**,**b** were obtained by comparing the area under the corrected emission spectrum of the test sample with that of a solution of Rhodamine 6G in methanol, which has a quantum yield of 94% according to the literature.[15] The relative quantum yields of **3** and **4** were obtained by using Cresyl Violet (54% in methanol)[16] and Nile Blue (26% in ethylene glycol),[17] respectively, as external references. For the fluorescence experiments, dilute solutions with an optical density of below 0.2 at the absorption maximum were used.

TPA measurements: The TPA spectra were determined by using laser pulses with a repetition rate of 80 MHz, a pulse duration of about 140 fs, and a wavelength range of $\lambda = 680$–1080 nm that was generated by a mode-locked Ti/sapphire laser (Chameleon Ultra II, Coherent, Inc.). All data were obtained in toluene (100 μM) by using the TPE fluorescence method with Rhodamine B (100 μM in methanol) as a reference.[23]

In vitro cellular imaging with tumor cells: HeLa cells (American Type Culture Collection, Manassas, VA) were cultured in minimum essential medium (MEM) supplemented with 10% fetal bovine serum (FBS), according to the instructions supplied by the vendor. The cells were trypsinized and resuspended in MEM alpha medium with 10% FBS at a concentration of 7.5×10^5 cells mL^{-1}, then plated in 35 mm culture plates by using 2.5 mL of medium that contained 0.10 mL of the cell suspension. The plates were incubated overnight at 37°C under a 5% CO_2 atmosphere. Then the cells (50% confluency) were carefully rinsed with phosphate-buffered saline (PBS), and the medium (2.0 mL), which contained the aqueous dispersion (80 μL) also containing solutions of selected compounds (10^{-4} M) in 2.5% DMSO, was added to plate and mixed gently. The treated cells were reincubated for 1 h. Then the plates were rinsed three times with sterile PBS, and fresh media were added. The cells were then directly imaged by using a Leica laser scanning confocal inverted microscope (TCS SP2, Leica Microsystems Semiconductor GmbH). This microscope was equipped with multiple visible laser lines ($\lambda=514$, 543, and 633 nm) for one-photon excitation and confocal imaging, and a Ti/sapphire laser (Chameleon Ultra II, Coherent, Inc.) for two-photon excitation ($\lambda=1028$ nm). The lightsource under the microscope was controlled by using neutral-density filters and was maintained at 10 mW for the two-photon imaging process. A 63.0× oil immersion objective (HCX PL APO CS, 63×, NA 1.40) was used for all cell-imaging processes. Three different imaging channels at $\lambda=520$–580, 600–690, and 710–780 nm were used for **2b**, **3**, and **4**, respectively, to remove the scattering influence from the excitation lights.

Acknowledgements

This work was supported in part by a grant from the Chemistry and Life Sciences Directorate of the Air Force Office of Scientific Research and in part by the John R. Oishei Foundation. Partial support from the Center of Excellence in Bioinformatics and Life Sciences at University at Buffalo is also acknowledged. We thank Dr. Shao-liang Zheng for obtaining the crystal structures and Dr. Hong Ding for providing the HeLa cells.

[1] A. S. Waggoner, L. Stryer, *Proc. Natl. Acad. Sci. USA* **1970**, *67*, 579–589.
[2] R. Y. Tsien, *Annu. Rev. Neurosci.* **1989**, *12*, 227–253.
[3] X. H. Fang, J. W. J. Li, J. Perlette, W. H. Tan, K. M. Wang, *Anal. Chem.* **2000**, *72*, 747A–753A.
[4] A. L. Tatarets, I. A. Fedyunyayeva, T. S. Dyubko, Y. A. Povrozin, A. O. Doroshenko, E. A. Temetschnig, L. D. Patsenker, *Anal. Chim. Acta* **2006**, *570*, 214–223.
[5] J. Fabian, H. Nakazumi, M. Matsuoka, *Chem. Rev.* **1992**, *92*, 1197–1226.
[6] M. Shah, K. Thangaraj, M. L. Soong, L. Wolford, J. H. Boyer, I. R. Politzer, T. G. Pavlopoulos, *Heteroat. Chem.* **1990**, *1*, 389–399.
[7] A. Loudet, K. Burgess, *Chem. Rev.* **2007**, *107*, 4891–4932.
[8] Z. Dost, S. Atilgan, E. U. Akkaya, *Tetrahedron* **2006**, *62*, 8484–8488.
[9] J. S. Li, H. Wang, L. W. Cao, H. S. Zhang, *Talanta* **2006**, *69*, 1190–1199.
[10] M. Kollmannsberger, K. Rurack, U. Resch-Genger, W. Rettig, J. Daub, *Chem. Phys. Lett.* **2000**, *329*, 363–369.
[11] W. Qin, M. Baruah, M. Van der Auweraer, F. C. De Schryver, N. Boens, *J. Phys. Chem. A* **2005**, *109*, 7371–7384.
[12] H. L. Kee, C. Kirmaier, L. H. Yu, P. Thamyongkit, W. J. Youngblood, M. E. Calder, L. Ramos, B. C. Noll, D. F. Bocian, W. R. Scheidt, R. R. Birge, J. S. Lindsey, D. Holten, *J. Phys. Chem. B* **2005**, *109*, 20433–20443.
[13] Z. Shen, H. Rohr, K. Rurack, H. Uno, M. Spieles, B. Schulz, G. Reck, N. Ono, *Chem. Eur. J.* **2004**, *10*, 4853–4871.
[14] N. Kuhn, A. Kuhn, M. Speis, D. Blaser, R. Boese, *Chem. Ber.* **1990**, *123*, 1301–1306.
[15] W. Baumler, A. Penzkofer, *Chem. Phys.* **1990**, *140*, 75–97.
[16] D. Magde, J. H. Brannon, T. L. Cremers, J. Olmsted, *J. Phys. Chem.* **1979**, *83*, 696–699.
[17] R. Sens, K. H. Drexhage, *J. Lumin.* **1981**, *24/25*, 709–712.
[18] T. R. Krishna, M. Parent, M. H. V. Werts, L. Moreaux, S. Gmouh, S. Charpak, A. M. Caminade, J. P. Majoral, M. Blanchard-Desce, *Angew. Chem.* **2006**, *118*, 4761–4764; *Angew. Chem. Int. Ed.* **2006**, *45*, 4645–4648.
[19] C. Stosiek, O. Garaschuk, K. Holthoff, A. Konnerth, *Proc. Natl. Acad. Sci. USA* **2003**, *100*, 7319–7324.
[20] H. J. Koester, D. Baur, R. Uhl, S. W. Hell, *Biophys. J.* **1999**, *77*, 2226–2236.
[21] Q. Zheng, T. Y. Ohulchanskyy, Y. Sahoo, P. N. Prasad, *J. Phys. Chem. C* **2007**, *111*, 16846–16851.
[22] P. N. Prasad, *Introduction to Biophotonics*, Wiley, New York, **2003**.
[23] C. Xu, W. W. Webb, *J. Opt. Soc. Am. B* **1996**, *13*, 481–491.
[24] M. D. Bowman, R. C. Jeske, H. E. Blackwell, *Org. Lett.* **2004**, *6*, 2019–2022.
[25] P. Madsen, A. Ling, M. Plewe, C. K. Sams, L. B. Knudsen, U. G. Sidelmann, L. Ynddal, C. L. Brand, B. Andersen, D. Murphy, M. Teng, L. Truesdale, D. Kiel, J. May, A. Kuki, S. Shi, M. D. Johnson, K. A. Teston, J. Feng, J. Lakis, K. Anderes, V. Gregor, J. Lau, *J. Med. Chem.* **2002**, *45*, 5755–5775.
[26] a) Bruker AXS, SMART and SAINTPLUS, Bruker AXS, Madison, Wisconsin (USA), **2006**; b) G. M. Sheldrick, SHELXS-97 and SHELXL-97, Bruker Analytical Instrumentation, Madison, Wisconsin (USA), **2000**.

Received: February 19, 2008
Published online: May 21, 2008

